Proceedings of ICFDP8:
Eighth International Congress of Fluid Dynamics & Propulsion
December 14-17, 2006, Sharm El-Shiekh, Sinai, Egypt
ICFDP8-EG-172

# Numerical calculation of particle separation in a cyclone flow using LES

H. Shalaby[1], K. Wozniak[2], G. Wozniak

[1] Laboratory of Fluid Mechanics and Technical Flows, University of Magdeburg 'Otto von Guericke', Universitätsplatz 2 D-39106 Magdeburg, Germany

[2] SIVUS gGmbH, Schulstr. 38 D-09125 Chemnitz, Germany

*Author for correspondence: guenter.wozniak@mb.tu-chemnitz.deChemnitz University of Technology, Chair of Fluid Mechanics, Straße der Nationen 62 D-09107 Chemnitz, Germany

**Abstract**

Numerical flow calculations were carried out at various axial positions of a gas cyclone separator for industrial applications. Due to the nature of cyclone flows, which exhibit highly curved streamlines and anisotropic turbulence, we used the advanced turbulence model Large Eddy Simulation (LES). The application of LES reveals better agreement with the experimental data, however, it requires higher computer capacity and longer running times when compared to standard turbulence models. The particle-laden flow of a cyclone separator for industrial applications at a Reynolds number of Re = 140,000 has been studied numerically. These calculations of the continuous phase flow were the basis for modeling the behavior of the solid particles in the cyclone. Particle trajectories, pressure drop and the cyclone separation efficiency have been studied in some detail.

The paper is organized into five sections. The first section consists of an introduction and a summary of previous work. Section 2 deals with LES turbulence modeling of the continuous phase flow. The third section treats modeling of the dispersed phase behavior. In section 4, computational issues are presented and discussed as applied grids, boundary conditions and the solution algorithm. In section 5, prediction profiles of the gas flow at axial positions are presented and discussed in some detail. Moreover, pressure drop, particle trajectories and cyclone efficiency are discussed here. Section 6 summarizes and concludes the paper.

1 Hemdan.Shalaby@vst.uni-magdeburg.de
2 Klaus.Wozniak@mbv.tu-chemnitz.de

## 1. Introduction

A cyclone separator is a device, which causes centrifugal separation of dispersed phase materials in a fluid flow. Unlike the slow settling of particles within a settling tank, a cyclone separator system yields fast separation and utilizes less space. Separation occurs fast because one “g” of the gravitational force is replaced by multiple “g” of the acting centrifugal force. The material to be separated can consist of solid particles or liquids, i.e. droplets, which are classified according to size, shape, and density. The cyclone utilizes the energy obtained from the fluid pressure gradient to create rotational fluid motion. This rotational motion causes the dispersed phase to separate relatively fast due to the strong acting forces. In widely used reverse flow cyclones of the cylinder on cone design type, gases spiral down from a tangential inlet towards the apex of a conical section, where the flow is reversed and the particles are collected in a vessel called hopper. The continuous phase (cleaned gas) then proceeds upward in an inner core flow towards the gas exit via the outlet tube. Cyclone designs have been developed over many years since their invention. Nowadays, there exist a large number of different types for various industrial applications. Many attempts have been made to improve the performance of cyclones by modifying their shape in terms of the ratio of different key dimensions. Generally, the continuous phase flow still carries a fraction of small particles when it proceeds upward in the inner flow core towards the gas exit. Therefore, a solid apex cone has been incorporated in the cyclone to slow down the flow inside the hopper and thus increase the separation efficiency.

Computational fluid dynamics CFD has become a widely accepted design tool for research and development in fluid mechanics over the last decade. However, the number of publications concerning experimental investigations of cyclone flows is still exceeding by far the number of published numerical investigations. In the past, mainly 2-dimensional analysis has been performed using radial symmetry of the flow in the cyclone, which in certain cases is an inadmissible simplification (Gorton-Huelgerth 1999). In recent years, much work dealing with 3-dimensional predictions of gas-particle flows in cyclone separators has been published. The results show that the quality of the numerical solutions strongly depends on the type of turbulence model applied to the continuous phase flow.

A 3-dimensional Eulerian-Lagrangian approach in (Minier et al. 1991) has been used applying a modified $k-\varepsilon$ turbulence model. The authors stated that the variations of the coefficients of restitution in the particle-wall model from elastic to completely inelastic

bouncing behavior have shown only minor influence on the predicted efficiency grade. Boysan et al. (1986) presented the theory of a 3-dimensional modified algebraic Reynolds stress turbulence model (ASM). They found good agreement between the predicted flow field in the investigated cyclone in the range of the so-called potential vortex and an at least qualitative agreement in the core region. The potential vortex appears between the free vortex close to the wall and the forced vortex close to the core. Gorton-Huelgerth (1999) performed 3-dimensional calculations for a series of standard cyclones using the commercial computer package FLUENT 4.4.7 and FLUENT UNS 4.2.10 (Fluent 1997) with a built-in Reynolds stress turbulence model (RSM). Several different cyclone geometries (e.g. variation of the hopper entrance geometry) have been investigated. Numerical results for the gas velocity field showed very good agreement with their Laser Doppler Anemometer (LDA) measurements. Frank et al. ( July 18-19,1997; 1998; June 22-26,1997; 1999) developed a 3-dimensional Eulerian-Lagrangian approach (MISTRAL/PartFlow-3D) for the numerical prediction of gas-particle flows. Special emphasis has been put on the parallelization of the numerical algorithm for the prediction of the continuous phase. Furthermore, the model is extended for the particle trajectory calculation in order to enable numerical predictions for disperse gas-particle flows in large and complex flow configurations of various industrial applications. Derksen (2002) presented a numerical prediction of a flow in a Stairmand high efficiency cyclone at a Reynolds number of Re = 280,000. He performed calculations using Large Eddy Simulation based on the Smagorinsky model. His results agree well with experimental data (LDA measurements of the average and RMS values of the tangential and axial velocity). Souza and Neto (2002) have used sub grid scale Smagorinsky modeling to predict the behavior of a water-fed hydro cyclone. The numerical results captured the main features of the flow pattern and agreed reasonably well with experiments. The authors suggested that LES represents an interesting alternative to classical turbulence models when applied to the numerical solution of fluid flows within hydro cyclones. Recently, Shalaby et al. (2005) carried out numerical calculations at the apex cone at various axial positions of a gas cyclone separator for industrial applications. Their work was based on the comparison between three turbulence models, $k-\varepsilon$, RSM (Reynolds Stress Models) and LES. The authors found that the application of the LES reveals a better qualitative agreement with the experimental data, but requires higher computer capacity and longer running times than RSM.

The objective of this paper is to investigate the following items by means of numerical investigation using LES: velocity profiles, pressure drop, particle trajectories and cyclone separation efficiency.

## 2. Large Eddy Simulation Model (LES)

LES requires the separation of small eddies from large eddies implementing a filter. For the sake of simplicity, the following section uses one-dimensional notations,

$$\overline{u_i} = \int G(x, x') u_i(x) dx' \tag{1}$$

where $\overline{u_i}$ and $G(x, x')$ denote the filter velocity and the top-hat filter function respectively. The filter function is large only when $G(x, x')$ is less than the filter width $\Delta_i$, a length scale, over which the averaging is performed. Flow eddies larger than the filter width $\Delta_i$ are defined as "large eddies" and eddies which are smaller than the width $\Delta_i$ are defined as "small eddies":

$$G(x_i) = \begin{cases} \dfrac{1}{\Delta_i} & |x_i| \le \dfrac{\Delta_i}{2} \\ 0 & |x_i| > \dfrac{\Delta_i}{2} \end{cases} \tag{2}$$

Using the finite volume method, it seems natural to define the filter width $\Delta_i$ as an average over a grid volume. Using this filter it is possible to derive the governing conservation equations for the momentum (Navier-Stokes equations) and mass continuity. The filtered Navier-Stokes equations in dimensionless form assuming incompressible flow can be written as:

$$\frac{\partial \overline{u_i}}{\partial x_i} = 0 \tag{3}$$

$$\frac{\partial \overline{u_i}}{\partial t} + \frac{\partial}{\partial x_j}\left(\overline{u_i}\,\overline{u_j}\right) = -\frac{\partial \overline{p}}{\partial x_i} + \frac{1}{Re}\frac{\partial^2 \overline{u_i}}{\partial x_j \partial x_j} - \frac{\partial \tau_{ij}}{\partial x_j} \tag{4}$$

Equations (3) - (4) govern the evolution of the large scales. The resulting effects of the small scales appear in the subgrid-scale stresses,

$$\tau_{ij} = \overline{u_i u_j} - \overline{u_i} \cdot \overline{u_j} \tag{5}$$

which must be modeled. Most of the existing models are of the eddy viscosity type and assume proportionality between the anisotropic part of the subgrid scale (SGS) stress tensor,

$$\tau_{ij}^{a} = \tau_{ij} - \delta_{ij}\tau_{kk}/3 \tag{6}$$

and the large-scale strain rate tensor, $\overline{S_{ij}}$:

$$\tau_{ij}^{a} = -2\upsilon_t \overline{S_{ij}} = -\upsilon_t \left( \frac{\partial \overline{u_i}}{\partial x_j} + \frac{\partial \overline{u_j}}{\partial x_i} \right). \tag{7}$$

The first SGS model was proposed by Smagorinsky (1963). It is based on the Boussinesq eddy-viscosity approximation that relates the turbulent shear stresses linearly to the strain rates. Equilibrium turbulence and isotropic sub-grid scales are assumed. Thus one can write

$$\tau_{ij} = -\upsilon_t S_{ij} \tag{8}$$

where the sub grid viscosity $\upsilon_t$ is defined as

$$\upsilon_t = 2(C_s \Delta)^2 \sqrt{2 S_{ij} S_{ij}} \tag{9}$$

with $C_s = 0.1$ being the so-called Smagorinsky constant, for details see (Denev 2003). The filter width $\Delta$ was calculated as $\Delta = (\Delta_x \Delta_y \Delta_z)^{\frac{1}{3}}$ according to (Denev 2003) to account for grid stretching in normal direction. The terms $\Delta_x$, $\Delta_y$ and $\Delta_z$ denote the mesh size in the x, y and z directions, respectively. The strain rate tensor is given by

$$\overline{S_{ij}} = \frac{1}{2} \left( \frac{\partial u_i}{\partial x_j} + \frac{\partial u_j}{\partial x_i} \right) \tag{10}$$

The Smagorinsky model depends only on large scales, which means that the model is generally too dissipative. Therefore, the model needs additional damping in the near-wall region. Otherwise no turbulent phenomena can be calculated by the algorithm. Consequently, a wall damping function has been applied according to (Launder and Spalding 1974),

$$f_\mu = 1 - \exp\left[ -\left( \frac{y^+}{A^+} \right)^3 \right] \tag{11}$$

with $A^+ = 25$ being the so-called *van Driest factor* (Van Driest 1965) and $y^+$ a dimensionless wall-coordinate (Launder 1975) defined by

$$y^+ = \frac{u_\tau y}{\upsilon} \tag{12}$$

where $u_\tau$ is the friction velocity, see (Smagorinsky 1963).

## 3. Motion of the Disperse Phase

The behavior of the disperse phase is described using the Lagrangian approach, i.e. discrete particle trajectories were calculated. Each calculated particle represents a large number of physical particles of the same physical properties, which was characterized by the particle flow rate $\dot{M}_P$ along each calculated particle trajectory. The prediction of the particle trajectories was carried out by solving the ordinary differential equations for the particle location, translational and rotational velocities. Assuming that the ratio of fluid $\rho_f$ to particle $\rho_p$ density is small, $(\rho_f/\rho_p) << 1$, these equations can be written as follows (Frank 1992; Tsuji et al. 1991)

$$\frac{d}{dt}\begin{bmatrix} x_p \\ y_p \\ z_p \end{bmatrix} = \begin{bmatrix} u_p \\ v_p \\ w_p \end{bmatrix} \tag{13}$$

$$\begin{aligned}
\frac{d}{dt}\begin{bmatrix} u_p \\ v_p \\ w_p \end{bmatrix} &= \frac{3}{4}\frac{\rho_f}{\left(\rho_p + \frac{1}{2}\rho_f\right) d_p} v_{rel} C_D(\mathrm{Re}_p) \begin{bmatrix} u_f - u_p \\ v_f - v_p \\ w_f - w_p \end{bmatrix} + \\
&+ \frac{v_{rel}}{\omega_{rel}} C_M(\sigma) \begin{bmatrix} (v_f - v_p)(\omega_z - \Omega_z) - (w_f - w_p)(\omega_y - \Omega_y) \\ (w_f - w_p)(\omega_x - \Omega_x) - (u_f - u_p)(\omega_z - \Omega_z) \\ (u_f - u_p)(\omega_y - \Omega_y) - (v_f - v_p)(\omega_x - \Omega_x) \end{bmatrix} \\
&+ \frac{2\upsilon_f^{1/2}}{\pi |\vec{\Omega}|^{1/2}} C_A \begin{bmatrix} (v_f - v_p)\Omega_z - (w_f - w_p)\Omega_y \\ (v_f - w_p)\Omega_x - (u_f - u_p)\Omega_z \\ (u_f - u_p)\Omega_y - (v_f - v_p)\Omega_x \end{bmatrix} \\
&+ \frac{\rho_p - \rho_f}{\rho_p + \frac{1}{2}\rho_f} \begin{bmatrix} g_x \\ g_y \\ g_z \end{bmatrix}
\end{aligned} \tag{14}$$

$$\frac{d}{dt}\begin{bmatrix}\omega_x\\ \omega_y\\ \omega_z\end{bmatrix} = -\frac{15}{16\pi}\frac{\rho_f}{\rho_p}\omega_{rel}\zeta_m\begin{bmatrix}\omega_x-\Omega_x\\ \omega_y-\Omega_y\\ \omega_z-\Omega_z\end{bmatrix} \tag{15}$$

With:

$$\begin{aligned}
&\mathrm{Re}_P = \frac{d_p v_{rel}}{\upsilon} \quad , v_{rel} = \sqrt{\left(u_f-u_p\right)^2+\left(v_f-v_p\right)^2+\left(w_f-w_p\right)^2} \quad ,\\
&\sigma = \frac{1}{2}\frac{d_p\omega_{rel}}{v_{rel}} \quad , \zeta_m = \zeta_m\left(\mathrm{Re}_\omega\right), \quad \mathrm{Re}_\omega = \frac{1}{4}\frac{{d_p}^2\omega_{rel}}{\upsilon},\\
&\vec{\Omega} = rot\vec{v}_f \quad , \omega_{rel} = \sqrt{\left(\omega_x-\Omega_x\right)^2+\left(\omega_y-\Omega_y\right)^2+\left(\omega_z-\Omega_z\right)^2}
\end{aligned} \tag{16}$$

In these equations the subscripts *p* indicates particle and *f* indicates the fluid, $\upsilon$ is the fluid kinematic viscosity, $d_p$ the particle diameter and $\omega_{rel}$ the absolute value of the relative rotational velocity between fluid and particle.

The equations of motion of the disperse phase include at the right hand side the following forces:

- Drag force.
- Lift force due to particle rotation (Magnus force).
- Lift force due to shear in the fluid flow field (Saffman force).
- The gravitational and added mass forces.

For a detailed discussion of the forces acting on a particle see for example Crowe et al**.** (Crowe et al. 1998)**.** For very fine particles in the particle diameter range of interest ($d_p$ < 10 µm and particle density $\rho_p$ = 2500 $kg/m^3$), the Magnus force due to particle rotation has been neglected since the particle diameter is very small. The values for the Coefficients $C_D, C_M, C_A$ *and* $\zeta_m$ and other model constants, e.g. restitution coefficients $k_w$ and coefficient of kinetic friction $f_W$ in the particle wall collision model can be found in (Frank 1992; Frank et al. 1997; Sommerfeld 1996), for example. The effect of fluid turbulence on the motion of the disperse phase is significant in the selected particle diameter range and therefore has been taken into account by using the Lagrangian Stochastic-Deterministic (LSD) turbulence model proposed in (Milojevic 1990).

### *3.1 Particle-Wall Collision Model*

In various industrial applications disperse multiphase-flows are confined by rigid boundaries. Especially the motion of large particles, which is dominated by inertia, is strongly influenced by the confinement. Considering the wall-collision process it has been shown that irregularities due to wall roughness and deviation of particle shape from a sphere play an important role (Frank 1992; Matsumoto et al. 1976; Tsuji et al. 1985). The particle-wall collisions were treated according to the irregular bouncing model by Sommerfeld (1992; 1996) in the modified wall roughness formulation given in (Frank 1992; Frank et al. 1997; Tsuji et al. 1991). In this model the particle collides with an inclined virtual wall. The inclination angle $\gamma$ is sampled from a Gaussian distribution with a mean value of $0^{o}$ and a standard deviation of $\Delta\gamma$. The latter depends on the particle diameter $d_p$ and the roughness parameters and may be estimated by:

$$\Delta\gamma = \arctan\frac{2\Delta H_r}{L_r} \quad for\ d_p \geq \frac{L_r}{\sin\left(\arctan\frac{2H_r}{L_r}\right)}$$

$$\Delta\gamma = \arctan\frac{2H_r}{L_r} \quad for\ d_p < \frac{L_r}{\sin\left(\arctan\frac{2H_r}{L_r}\right)} \tag{17}$$

Where

- $L_r$ is the mean cycle roughness.
- $H_r$ is the mean roughness height.
- $\Delta H_r$ is the standard deviation of the roughness height.

Since no preferential direction of roughness is assumed, the inclined virtual wall is additionally turned around with respect to the normal vector of the original wall by an azimuthal angle $\sigma_a$. This angle is sampled from a uniform distribution in the range $[-\pi, \pi]$.

The particle velocity and angular velocities were transformed to a coordinate system that is aligned with the collision plane. In the following equations it is assumed that the y-axis of the transformed coordinate system is identical to the normal vector of the collision plane. The computation of the velocities and angular velocities after rebound was carried out by

applying the impulse equations and taking into account the type of collision, i.e. sliding or non-sliding collision (Tsuji et al. 1991):

- Sliding collision: $-\frac{2}{7 f_W (k_W + 1)} \le \frac{v_p^{(1)}}{|v_r|} \le 0$ :

$$
\begin{aligned}
u_p^{(2)} &= u_p^{(1)} + \varepsilon_x f_W (k_W + 1) v_p^{(1)} \quad , \\
v_p^{(2)} &= -k_W v_p^{(1)} \quad , \\
w_p^{(2)} &= w_p^{(1)} + \varepsilon_z f_W (k_W + 1) v_p^{(1)} \quad , \\
\omega_x^{(2)} &= \omega_x^{(1)} - \frac{5}{d_p} \varepsilon_z f_W (k_W + 1) v_p^{(1)} \quad , \\
\omega_y^{(2)} &= \omega_y^{(1)} \quad , \\
\omega_z^{(2)} &= \omega_z^{(1)} + \frac{5}{d_p} \varepsilon_x f_W (k_W + 1) v_p^{(1)}
\end{aligned}
\tag{18}
$$

- Non-sliding collision: $\frac{v_p^{(1)}}{|v_r|} < -\frac{2}{7 f_W (k_W + 1)}$ :

$$
\begin{aligned}
u_p^{(2)} &= \frac{5}{7}\left( u_p^{(1)} - \frac{d_p}{5} \omega_z^{(1)} \right) \quad , \\
v_p^{(2)} &= -k_W v_p^{(1)} \quad , \\
w_p^{(2)} &= \frac{5}{7}\left( w_p^{(1)} + \frac{d_p}{5} \omega_x^{(1)} \right) \quad , \\
\omega_x^{(2)} &= \frac{2}{d_p} w_p^{(1)} \quad , \\
\omega_y^{(2)} &= \omega_y^{(1)} \quad , \\
\omega_z^{(2)} &= -\frac{2}{d_p} u_p^{(1)} \quad ,
\end{aligned}
\tag{19}
$$

with:

$$
|v_r| = \sqrt{\left( u_p^{(1)} + \frac{d_p}{2} \omega_z^{(1)} \right)^2 + \left( w_p^{(1)} - \frac{d_p}{2} \omega_x^{(1)} \right)^2}
$$

and:

$$
\varepsilon_x = \frac{u_p^{(1)} + \frac{d_p}{2} \omega_z^{(1)}}{|v_r|}, \quad \varepsilon_z = \frac{w_p^{(1)} - \frac{d_p}{2} \omega_x^{(1)}}{|v_r|}
$$

In these equations $k_W$ is the coefficient for restitution and $f_W$ the coefficient of kinetic friction, which can be obtained from (Frank 1992). The superscripts (1) and (2) indicate values before and after collision, respectively.

## 4. Computational Parameters

Due to the complex geometry of the cyclone a first guess numerical grid with 80 different grid blocks and about 660,000 finite volume elements had to be designed for first numerical calculations of the continuous phase flow. It will be referred to the first numerical grid as coarse grid. In a second numerical investigation the numerical grid was redesigned using the grid generator ICEM/CFD-HEXA (GmbH. 1998) with 80 grid blocks, about 1,300,000 finite volume elements, which will be referred to as fine uniform grid, Fig. 1a. The design of the control volumes was important for several reasons. First of all the control volumes had to be small enough to be able to resolve the significant length scale of the flow. In general this means that a more complex flow with large gradients needs more cells, i.e. a higher cell density in order to capture the correct flow field. More cells will on the other hand lead to a computationally larger problem and require more CPU- time. A compromise is to generate a more dense mesh where large gradients are expected, to increase the mesh size, and to decrease the total number of cells in areas where the flow calculation is less sensitive to the cell size. The mesh size variation has been limited by a factor of 5 to ensure a smooth solution. Grid refinement was applied at the gas inlet and to the region in the vicinity of the lower end of the gas exit tube.

Boundary conditions were used at the inlet, which means that the values of the variables are specified. The Reynolds number is about 140,000 at the inlet duct based on the hydraulic diameter and the bulk velocity. For the sake of simplicity a laminar velocity profile was assumed at the inlet area. In reality, the inlet flow is not laminar (Re = 140,000). However, the results are insensitive to the inlet velocity profile as shown in (Derksen 2002).

The conservation equations of fluid motion are solved by using LES with the MISTRAL-3D code (Vazquez and Métais 2002). The code is based on a finite volume approach, implicit time steps, the SIMPLE (Patankar 1980) algorithm for velocity-pressure coupling and a second-order central-differencing scheme (CDS) for convection. The solution procedure is based on a geometrical multigrid for improved convergence of pressure-velocity coupling on large numerical grids.

Computational results presented in this paper have been performed on sub clusters of 40 processors of the Chemnitz Linux Cluster CLIC (528 Intel / Pentium III, 800 MHz, 512 Mb RAM per node, 2 x FastEthernet), see (CLIC 1998). The calculations on the PC clusters were performed using a Message Passing Interface (MPI) distribution of LAM-MPI 6.3.5. The CPU-time for the investigation (35 000 time steps) was 242 hours and the parallel efficiency (the ratio of speed up to the number of processors) achieved amounts 0.74. On average, 5 iterations of the SIMPLE algorithm within one time step were performed.

Initially, 500 consequently decreasing time steps were performed in order to allow the cyclone flow to reach a fully developed state. The time step reached after the initial iterations was $10^{-4}$ s real (physical) time. This time was kept constant during the rest of the computations. The averaging process was started after the initial iterations and all mean characteristics of the flow have been obtained after averaging over 35 000 time steps. The averaging in the present study was done only with respect to time. The CFL number which defines the relation between the temporal and spatial discretization accuracy was 0.85,

$$\mathrm{CFL} = \Delta t \max_{(x,y,z)} \left( \frac{\left|\overline{u}\right|}{\Delta_x} + \frac{\left|\overline{v}\right|}{\Delta_y} + \frac{\left|\overline{w}\right|}{\Delta_z} \right) \tag{20}$$

Moreover, a second order accurate implicit time scheme was used in the study for temporal discretization.

In order to study the particle trajectories and collection efficiency of the cyclone, particles were released in the LES flow field. The particles were considered to be points in space that experience gravity, drag and lift forces. One-way coupling (effect of turbulence on particle trajectories) was assumed.

## 5. Results and Discussions

### *5.1 Velocity Profiles*

The investigated cyclone separator is characterized by the geometrical properties shown in Fig. 1b. Comparisons have been made between the calculated and measured axial and tangential velocity profiles at different horizontal cut planes in dimensionless form in

(Shalaby et al. 2005). The dimensionless velocity profile is scaled with the inlet duct velocity. The experimental data used for validation are published in (Fraser et al. 1997). In Fig. 2 the predicted and measured tangential velocity profiles of the continuous phase flow of cut plane 1 (left) and 2 (right) are shown. The measured profiles show that the central region in the cyclone rotates like a solid body where the tangential velocity is increasing with an increasing radius. The maximum tangential velocity of approximately 1.24 and 1.25 respectively times the inlet velocity is reached at approximately 25% of the radius from the center of the cyclone. Then, the tangential velocity starts to decrease and reaches zero velocity at the wall. Comparison with the experimental data shows, that LES predicts the shape of the tangential velocity profile with higher accuracy when compared to $k-\varepsilon$ turbulence model results (Agee and Gluhovsky 1999).

In Fig. 3 the predicted and measured axial velocity profiles are shown at cut plane 1 (left) and 2 (right). A value of zero on the radial axis characterizes the center of the cyclone. Positive velocities are directed upward towards the outlet. Both, measurements and predictions show the typical axial velocity profiles of a cyclone. There is an outer region close to the wall of the cyclone where the flow is directed downwards. The maximum axial velocities are found in the center of the cyclone where the flow is directed upwards with 1.1 and 1.2 respectively times the inlet velocity. At slightly more then half of the cyclone radius the flow direction reverses. The maximum axial velocities of the experiment are found equal to the inlet velocity (Breuer 1998). It is shown that also here LES predicts the axial velocity profile in satisfying agreement with experimental data of (Chiesa et al. 2005) as shown in Fig. 3.

### *5.2 Pressure Drop*

The pressure drop between the inlet and outlet has been predicted from the results obtained with LES using a fine grid. These computations have been carried out for various gas inlet velocities and the results are compared to the experimental data of (König 1990) . Fig. 4 shows the predicted total pressure drop compared to the experimental data. The numerical results of LES are in satisfying agreement with the experiments. The difference between LES and the experiments are of the order of 2 %. From comparison between the experimental and predicted total pressure loss across the cyclone, we can conclude that LES is an appropriate tool for the modeling of flow within the cyclone.

### *5.3 Particle trajectories.*

Fig. 5 shows examples of particle trajectories in the cyclone with an inlet gas velocity of 20 m/s. Fig. 5a shows a small particle of 0.5 μm in diameter, which is captured by the secondary flow along the cyclone top cover and follows the secondary flow along the wall of the vortex finder tube to the outlet gas exit. Fig. 5b shows a 1.0 μm particle moving along the outer conical wall going to the particle hopper. Because of its small size and thus low inertia it cannot be separated. It follows the recirculating gas flow back into the cyclone body where it is captured into the vortex core and moves upward to the outlet gas exit. A slightly larger particle of 1.3 μm in Fig. 5c is first captured in a particle rope along the cyclone lid. However, it is too large to follow the recirculating flow to the vortex finder tube. Therefore, it can be separated and moves down to the particle hopper where it is collected.

### *5.4 Cyclone separation efficiency.*

Separation efficiency is defined as the fraction of particles of any given size that are retained by the cyclone. The prediction of the particle separation efficiency has been carried out in accordance to (König 1990) . The quartz dust used as particle material had a particle diameter distribution in the range of $d_p$ = 0 to 50 μm with a mean particle diameter of 10.9 μm. The numerical computations were carried out for 20 particle diameter classes in the range between 0.5 and 15 μm. A particle density of 2500 kg/m$^3$ was assumed. The coefficients of restitution and kinetic friction values are 0.8 and 0.35, respectively, taken from reference (Frank et al. 1998). With an inlet gas velocity of 20 m/s, a series of separation rate computations were performed. The separation rate can be predicted as:

$$T(d_P) = 1 - \frac{\dot{N}_{out}(d_P)}{\dot{N}_{in}(d_P)} \tag{21}$$

where $\dot{N}_{in}(d_P)$ and $\dot{N}_{out}(d_P)$ are the particle flow rates for a given particle size in the inlet cross section and gas exit cross section respectively. The particle is assumed to be separated by the cyclone, if one of the following criteria are fulfilled:

i) the particle trajectory reaches the inlet cross section of the particle hopper.

ii) the particle sticks to the wall of the cyclone.

iii) the particle residence time in the cyclone is larger than the maximum allowed computations time.

Fig. 6 shows the comparison of the predicted separation efficiency with the experimental results of (König 1990) at a typical gas inlet velocity of 20 m/s. The figure presents satisfying agreement between LES and experimental results. The shape of the efficiency curve displays at least qualitatively the trend of the experimental data, however, the numerical results are somewhat shifted towards lower particle diameters.

## 6. Coclusions

The nature of the gas flow of a cyclone particle separator is highly swirling with anisotropic turbulence. Therefore, advanced turbulence models such as LES have to be applied to predict the gas flow behaviour. The LES results in case of the complex flow in a cyclone separator compare well with the experimental data found in the literature. This is one key result of our investigations. Therefore, the LES results are very encouraging and have shown that this model is a better alternative to conventional turbulence modelling of cyclone separator flows even when using a coarse-grid (Shalaby et al. 2005). The dynamic behaviour of the flow has been captured providing important information on the flow structure within the cyclone.

Also, the LES results of the continuous phase flow formed the basis for modelling solid particle motion in the cyclone based on one-way coupling between the gas flow field and the disperse phase. The pressure drop inside the cyclone has been studied at a fine grid for various gas inlet velocities. The difference between LES and available experimental pressure drop data is specifically around 2 %. Sample particle trajectories in the cyclone with an inlet particle velocity of 20 m/s have been presented and discussed.

In the flow field, solid particles of various sizes are released to predict the cyclone separation efficiency. Here, one-way coupling between the gas and the particles was assumed. The predicted cyclone separation efficiency results of LES show satisfying agreement with experimental data.

With these results, the potential of the LES model to simulate flows in a cyclone separator has been distinctly demonstrated. Eventually, we hope that this work will contribute to an improved understanding of the flow and separation process within cyclone separators in

order to optimise their technical concepts and encourages researchers to apply LES to calculate particle separation processes.

## References


Agee, E. M., and Gluhovsky, A. (1999). "LES model sensitivities to domains, grids, and large-eddy timescales." *Journal of the Atmospheric Sciences*, 56(4), 599-604.

Boysan, F., Swithenbank, J., and Ayers, W. H. (1986). " Mathematical Modelling of Gas-Particle Flows in Cyclone Separators." Encyclopedia of Fluid Mechanics, Gulf Publishing Company, Houston, Texas.

Breuer, M. (1998). "Large eddy simulation of the subcritical flow past a circular cylinder: Numerical and modeling aspects." *International Journal for Numerical Methods in Fluids*, 28(9), 1281-1302.

Chiesa, M., Mathiesen, V., Melheim, J. A., and Halvorsen, B. (2005). "Numerical simulation of particulate flow by the Eulerian-Lagrangian and the Eulerian-Eulerian approach with application to a fluidized bed." *Computers and Chemical Engineering*, 29(2), 291-304.

CLIC. (1998). "Chemnitz University of Technology." *http://www.tu-chemnitz.de/urz/anwendungen/CLIC*, Germany.

Crowe, C., Sommerfeld, M., and Tsuji, Y. (1998). *Multiphase Flows with Droplets and Particles.*, CRC Press, New York.

Denev, J., Frank, T., Pachler, K. (2003). "Large Eddy Simulation (LES) of Turbulent Square Channel Flow Using a PC-Cluster Architecture." *4th International Conference on Large-scale Scientific Computations*, 1 - 11.

Derksen, J. (2002). "LES - Based Separation Performance Predictions of A Stairmand Cyclone." *10th Workshop on Two - Phase Flow Predictions,Martin - Luther-Universität Halle - Wittenberg,* 9 - 12 April, *Halle (Saale), Germany*, 217-226.

Fluent. (1997). "Fluent User Guide Documentation."

Frank, T. (1992). "Numerische Simulation der feststoffbeladenen Gasströ.mung im horizontalen Kanal unter Berücksichtigung von Wandrauhigkeiten." *Freiberg Unversity of Mining and Technology, Dissertation, Germany*.

Frank, T., and Wassen, E. (1997) " Parallel Efficiency of PVM- and MPI-Implementations of two Algorithms for the Lagrangian Prediction of Disperse Multiphase Flows." *ISAC '97 Conference on Advanced Computing on Multiphase Flow*, Tokyo, Japan.

Frank, T., Wassen, E., and Yu, Q. (1998)"Lagrangian Prediction of Disperse Gas-Particle Flow in Cyclone Separators." *ICMF '98 -3rd International Conference on Multiphase Flow, June 8.-12. CD-ROM Proceedings, Paper No. 217*, Lyon, France.

Frank, T., Wassen, E., and Yu, Q. (1997) " A 3-dimensional Lagrangian Solver for Disperse Multiphase Flows on Arbitary, Geometricaly Complex Flow Domains using Block structured Numerical Grids." *Proceedings of the 7th Int. Symposium on Gas-Particle Flows*, June 22-26,Vancouver, BC, Canada.

Frank, T., Yu, Q., Wassen, E., and Schneider, J. (1999). "Experimental and numerical investigation of particle separation in a symmetrical double cyclone separator." *Proceedings of the 1999 3rd ASME/JSME Joint Fluids Engineering Conference, FEDSM'99, San Francisco, California, USA, 18-23 July*.

Fraser, S. M., Abdel Razek, A. M., and Abdullah, M. Z. (1997). "Computational and experimental investigations in a cyclone dust separator." *Proceedings of the Institution*

*of Mechanical Engineers, Part E: Journal of Process Mechanical Engineering*, 211 E4(E4), 247-257.
GmbH, ICEMCFD (1998). *ICEM/CFD Hexa Manual Documentation*.
Gorton-Huelgerth, A. (1999). "Messung und Berechnung der Geschwindigkeitsfelder und Partikelbahn im Gaszyklon.."
König, C. (1990). "Untersuchungen zum Abscheidverhalten von geometrisch ںhnlichen Zyklonen." *Dissertation, Unversity of Kaiserslautern, Germany*.
Launder, B., Reece, G., and Rodi, W. (1975). "Progress in the development of a Reynolds-Stress turbulence closure." *J. Fluid Mech.*, 68, 3, 537-566.
Launder, B. E., and Spalding, D. B. (1974). "The Numerical Computation of Turbulent Flows." *Computer Methods in Applied Mechanics and Engineering*, 3(2), 269-289.
Matsumoto, S., Saito, S., and Maeda, S. (1976). "Simulation of gas-solid two-phase flow in horizontal pipe." *Journal of Chemical Engineering of Japan*, 9(1), 23-28.
Milojevic, D. (1990). "Lagrangian Stochastic-Deterministic (LSD) Prediction of Particle Dispersion in Turbulence." *Part. Syst. Charact.*, 7, 181-190.
Minier, J. P., Simonin, O., and Gabillard, M. (1991). "Numerical modelling of cyclone separators." *Proceedings of the International Conference on Fluidized Bed Combustion, Quebec, Canada, April*, 3, 1251-1259.
Patankar, S. V. (1980). *Numerical Heat Transfer and Fluid Flow*, McGraw Hill, New York.
Shalaby, H., Pachler, K., Wozniak, K., and Wozniak, G. (2005). "Comparative study of the continuous phase flow in a cyclone separator using different turbulence models." *International Journal for Numerical Methods in Fluids*, 48(11), 1175-1197.
Smagorinsky, J. (1963). "General Circulation Experiment with the primitive equations." *Mon. Weather Rev.*, 91, 99-164.
Sommerfeld, M. (1992). "Modelling of Particle-wall collision in confined gas-particle flows." *Int. Journal of Multiphase Flows*, 18(6), 905-926.
Sommerfeld, M. (1996). "Modellierung und numerische Berechnung von partikelbeladenen turbulent Strö mungen mit Hilfe des Euler/Lagrange-Verfahrens." Berichte aus der Strö mungtechnik, Aachen, Germany.
Souza, F., and Neto, A. (2002)."Large Eddy Simulations of a hydrocyclone." *Proceedings of FEDSM ASME Fluid Engineering Division Summer Meeting, Montreal*, 14 - 18 July ,Quebec, Canada, 1 - 6.
Tsuji, Y., Shen, N. Y., and Morikawa, Y. (1985). "Numerical Simulation of penumatic conveying in a horizontal Pipe." *KONA - Powder Science and Technology in Japan*, 3, 38-51.
Tsuji, Y., Shen, N. Y., and Morikawa, Y. (1991). "Lagrangian Simulation of Dilute Gas-Solid Flows in a Horizontal Pipe." *Advanced Powder Technology*, 2(1), 63-81.
Van Driest, E. R. (1965). "On the Turbulent Flow over a Wall." *J. Aeronautical Science*, 23, 1007 - 1011.
Vazquez, M. S., and Métais, O. (2002). "Large-eddy simulation of the turbulent flow through a heated square duct." *J. Fluid Mech.*, 453, 201-238.

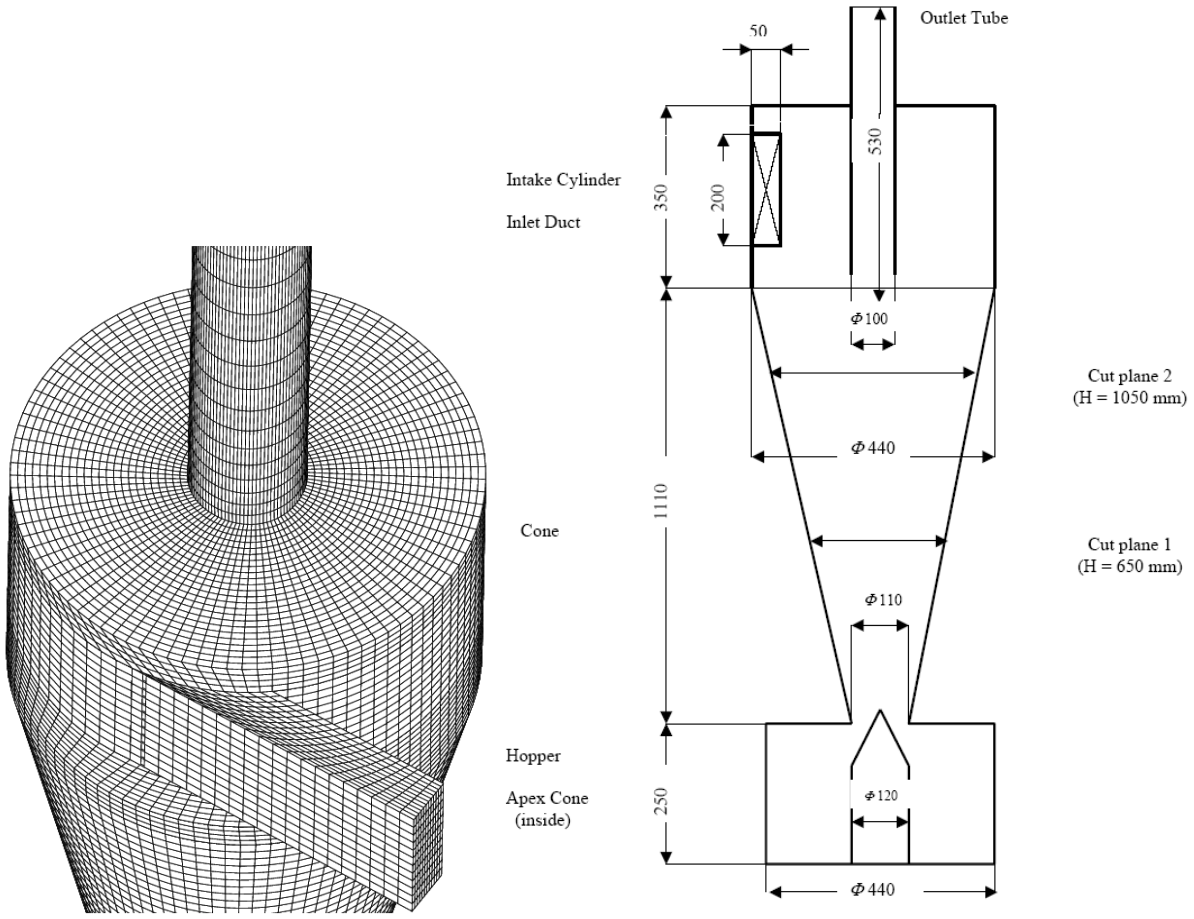


Fig. 1: Computational grid with 1,3 million finite volume elements (a) and location of different cut planes (b).

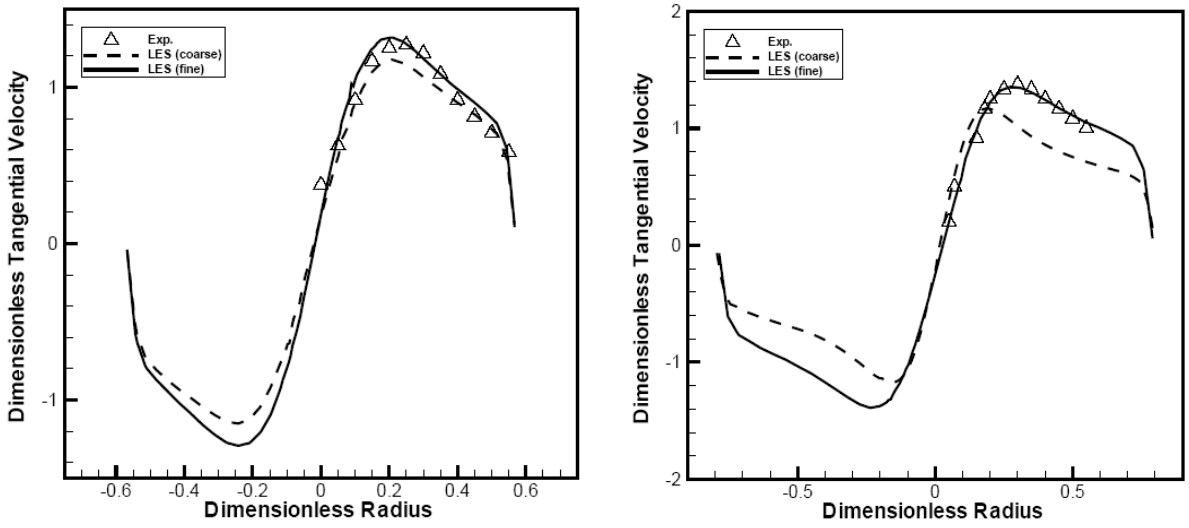


Fig. 2. Comparison of LES model and experimental data of (Fraser et al. 1997), tangential velocities at cut plane 1 (left) and 2 (right).

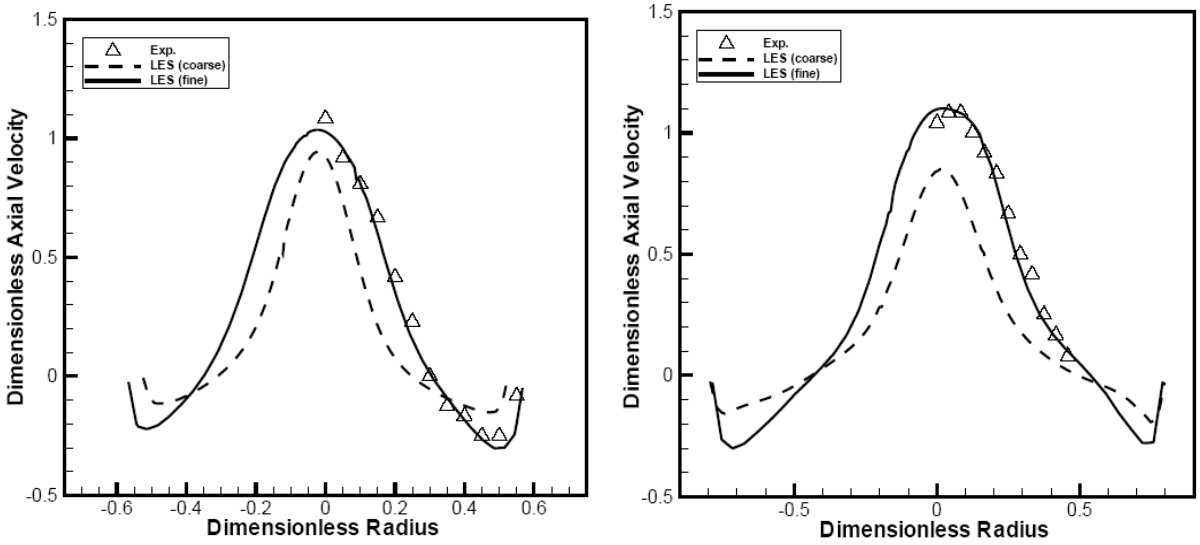


Fig. 3. Comparison of LES model and experimental data of (Fraser et al. 1997), axial velocities at cut plane 1 (left) and 2 (right).

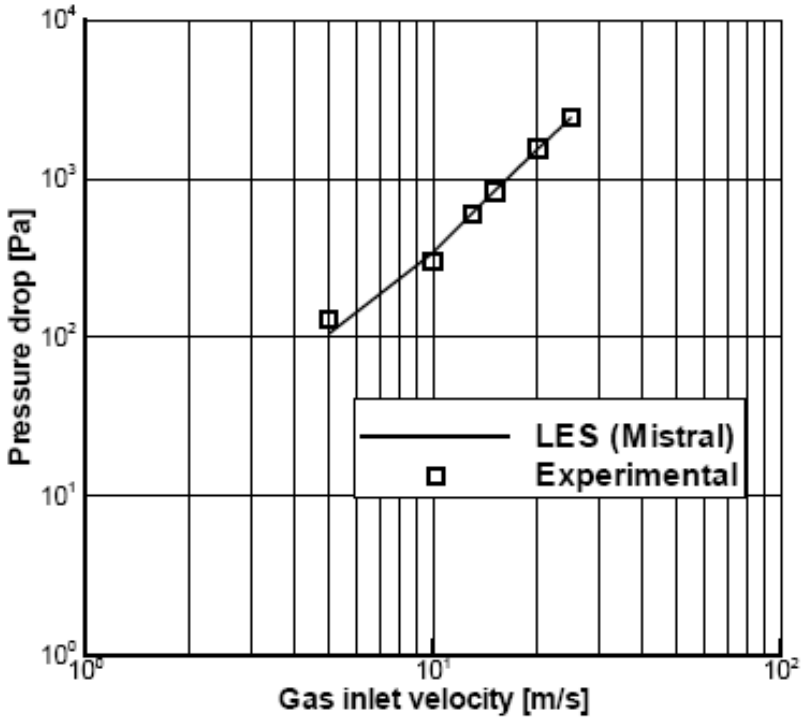


Fig. 4. Comparison of predicted pressure loss in the cyclone for various inlet velocities with experimental data of (König 1990).

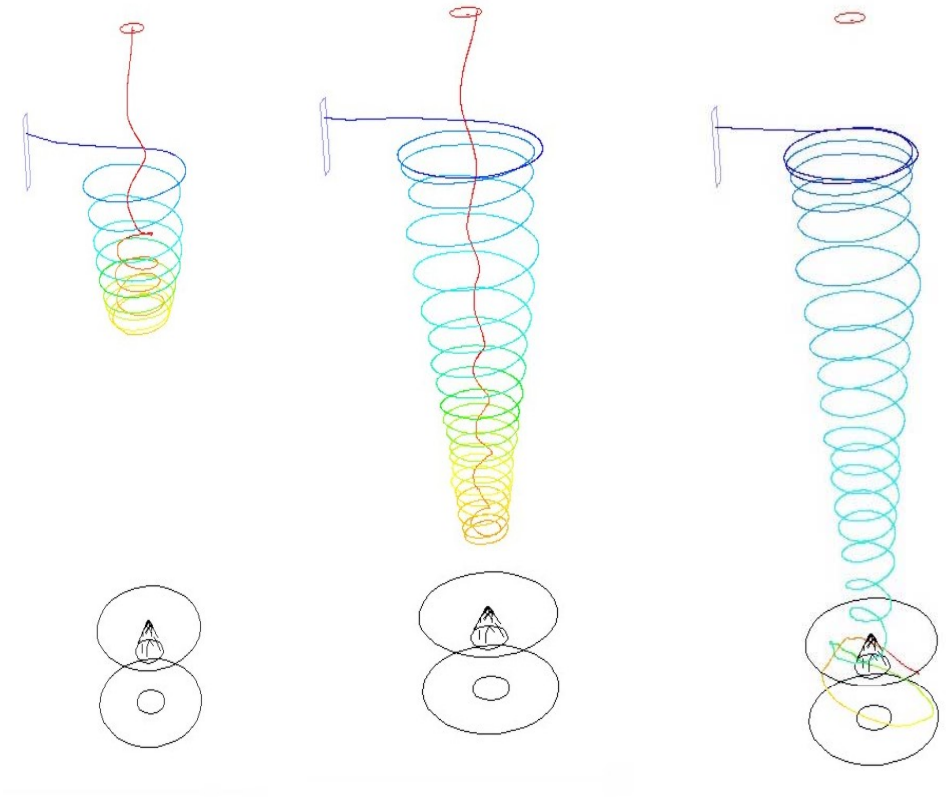


Fig. 5. Particle trajectories at different particle diameters of 0.5 (a), 1.0 (b) and 1.3 (c) μm. The colour distributions represent particle residence times (increase from blue to red).

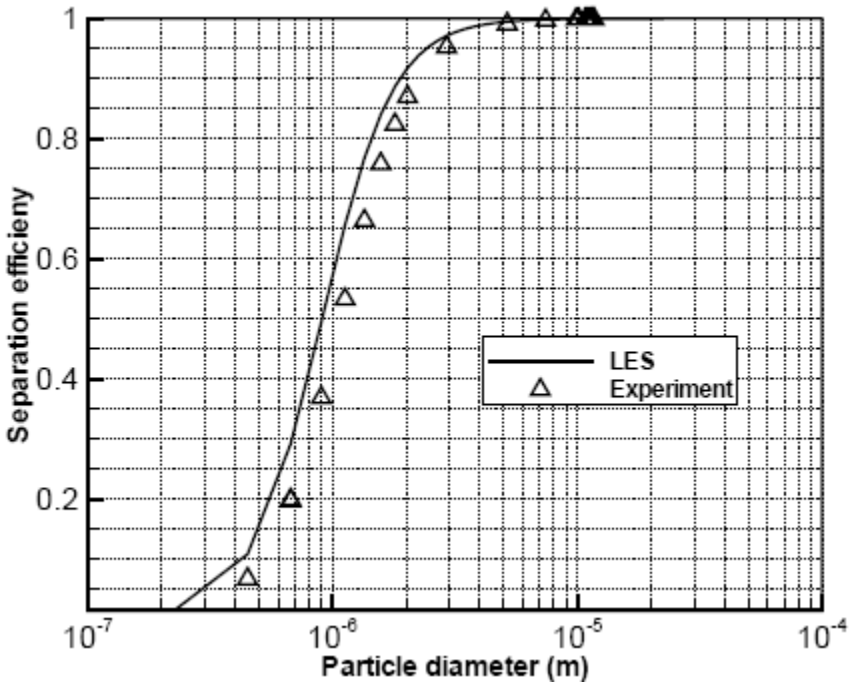


Fig. 6. Comparison of predicted cyclone separation efficiency with experimental data of (König 1990).